# Spectral tunability and enhancement of molecular radiative emission by metal-dielectric-metal stratified plasmonic nanostructure

Sepideh Golmakaniyoon, Pedro Ludwig Hernandez-Martinez, Hilmi Volkan Demir, and Xiao Wei Sun

**Articles you may be interested in**

# Spectral tunability and enhancement of molecular radiative emission by metal-dielectric-metal stratified plasmonic nanostructure

Sepideh Golmakaniyoon,[1,2] Pedro Ludwig Hernandez-Martinez,[2,3] Hilmi Volkan Demir,[1,2,3,a)] and Xiao Wei Sun[1,4,a)]

[1]*School of Electrical and Electronic Engineering, Nanyang Technological University, Singapore 639798*
[2]*LUMINOUS! Center of Excellence for Semiconductor Lighting and Displays, School of Electrical and Electronic Engineering, Nanyang Technological University, Singapore 639798*
[3]*Division of Physics and Applied Physics, School of Physical and Mathematical Sciences, Nanyang Technological University, 21 Nanyang Link, Singapore 637371*
[4]*Department of Electrical and Electronic Engineering, College of Engineering, Southern University of Science and Technology, 1088 Xue-Yuan Road, Shenzhen, Guangdong 518055, China*

Plasmonic nanostructures have been widely known for their notable capability to enhance spontaneous emission of an electric dipole in their vicinity. Due to the availability of large optical density of states at their metallic surface, the radiative and nonradiative decay channels are dramatically modified. However, enhancement cannot be realized for any desired emissive dipole as the plasmonic resonance frequency is mostly determined intrinsically by the existing plasmonic materials. Although recent studies using metamaterial structures demonstrate a promising approach of tuning the Purcell factor across the emission wavelength, many of the demonstrations lack efficient radiative emission besides the fabrication complexity. Here, we show theoretically and experimentally that a simple metal-dielectric-metal stratified architecture allows for high tunability of the resonance frequency to obtain a maximum radiative decay rate for any desired dipole peak emission wavelength. Owing to the effective cascaded plasmonic mode coupling across the metal-dielectric interfaces, the proposed approach uniquely provides us with the ability to optimize the plasmonic nanostructure for 100% radiative transmission and 3-fold radiative emission enhancement. *Published by AIP Publishing.* [http://dx.doi.org/10.1063/1.4985337]

In recent years, planar plasmonic nanostructures have attracted increasing attention thanks to their crucial role in the theoretical comprehension of surface enhanced fluorescence (SEF),[1] along with their wide applications in plasmonic waveguided mode nanostructures,[2] Raman scattering spectroscopy,[3–5] colour filters,[6,7] energy transfer,[8–11] and light-emitting and -harvesting devices.[12–17] It has been well understood that excitation of the surface plasmon (SP) modes at the surface of a metal gives rise to optical behaviour modification of a molecule in the vicinity of the metal surface due to the large enhancement of the local electromagnetic field.[18–23] More specifically, near-field coupling of the SP modes of a metal surface with the evanescent emission of light emitters leads to a large Purcell factor and enhanced spontaneous emission.[24–27] This effect offers the opportunity to manipulate the radiative and nonradiative decay rates of an emitter near metallic nanostructures as a result of the large optical density of states (DOS) available at their metal-dielectric interfaces.[18,28–31] However, despite the fact that several studies have reported significant enhancement of the fluorescence spontaneous emission rate, mostly the radiative decay rate contribution in the total relaxation rate has been suppressed by an extremely large nonradiative decay rate.[27,32] Also, the excitation enhancement plays a considerable additional role in increasing the fluorescence intensity.[26,33–35] In planar nanostructures, the constructive interference between incoming and reflected excitation electromagnetic waves results in the excitation field enhancement and consequently raises the fluorescence emission while the quantum yield is not improved.

The radiative emission enhancement is also affected by the spectral overlap between the SP modes and molecular emission spectra.[24] This overlap is essential to derive efficient SP coupling. Since this is possible for a limited number of existing materials, e.g., most commonly silver and gold in the visible, the radiative decay rate modification has been constrained to certain frequencies. From the discussion above, in order to realize a plasmonic structure benefiting from the enhanced radiative emission, it is therefore critical not only to enhance the radiative decay rate independent of the excitation pump but also to be able to adjust the resonance coupling frequency at any desired emission wavelength. Herein, we present theoretical and experimental demonstrations of the ability to tune surface plasmon modes to achieve the maximum radiative decay rate frequency of an emitting dipole in the vicinity of a simple stratified metal-dielectric-metal structure. This is enabled by efficient SP coupling at the metal-dielectric interfaces, which leads to the highest electric field enhancement at the dipole position in such an optimized cascade nanostructure. The results show ∼100% transmission of the dipole emission peak through an optimal structure. The design principle allows for modifying the proposed geometry to obtain a maximum transmission efficiency at any desired frequency. The current approach uniquely provides us with the ability to reach the highest plasmonic mode coupling to the far-field emission at the interfaces by adjusting variable geometrical parameters including the dielectric layer thickness.

---

a)Authors to whom correspondence should be addressed: hvdemir@ntu.edu.sg and sunxw@sustc.edu.cn
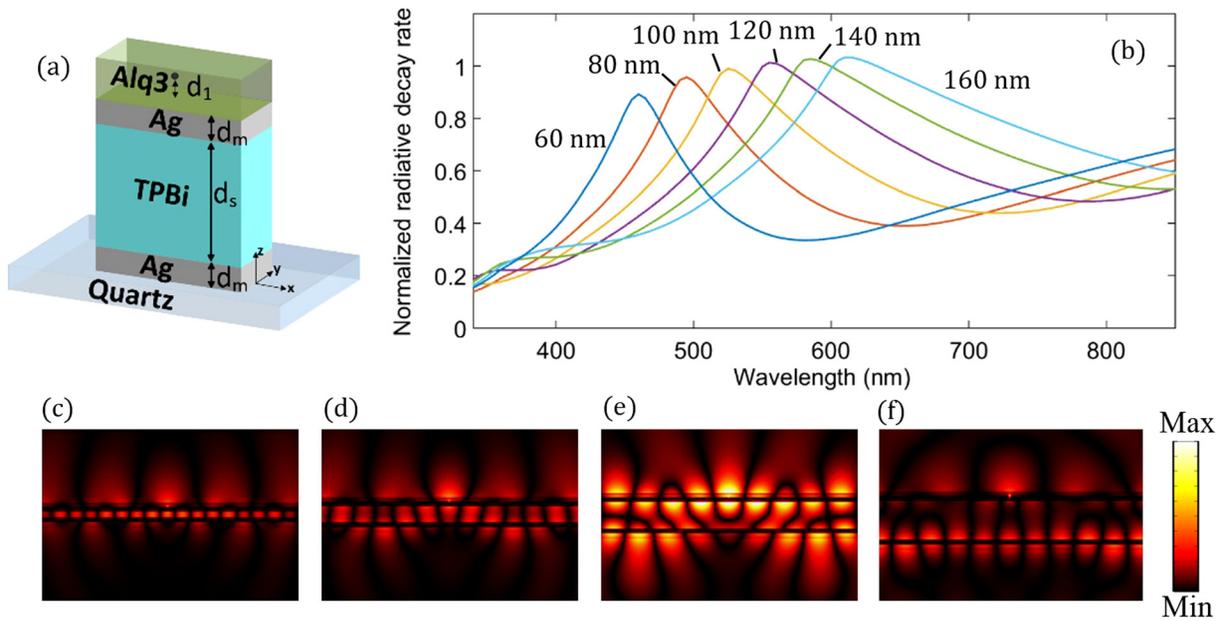
FIG. 1. (a) Schematic configuration of the proposed metal-dielectric-metal stratified structure deposited on a quartz substrate with Alq3 as an emissive layer on top of the plasmonic structure. The thickness of silver films is 20 nm and the spacer layer (TPBi) thickness varies from 40 to 200 nm to reach a resonance condition. (b) Radiative decay rate of an emitting dipole in front of the stratified structure (normalized to the maximum rate) versus emission peak wavelength for 60, 80, 100, 120, 140, and 160 nm thick spacer layers. (c)–(f) Calculated electric field distribution ($|E_z|$) in the stratified structure with the spacer layer thickness of 20 nm in (c), 60 nm in (d), 100 nm in (e), and 140 nm in (f) for an emitting dipole at the emission wavelength of 525 nm. The emissive layer is placed at the top half space surrounded by the dielectric medium.

Figure 1(a) presents the schematic view of the proposed configuration in which a thin film of an emissive layer [Tris (8-hydroxyquinolinato) aluminum, Alq3] was deposited on the layered metal-dielectric-metal plasmonic structure. This stratified structure consists of an optimized thickness of TPBi [2,2′,2″-(1,3,5-Benzinetriyl)-tris(1-phenyl-1-H-benz-imidazole)] that is sandwiched between two silver (Ag) films. The thickness of TPBi is determined through numerical computation to achieve a maximum transmission/radiative efficiency level at the desired emission frequency where the SP mode coupling leads to the highest radiative emission. In the numerical simulation, an emitting dye molecule was modelled as a Hertzian dipole located at 5 nm distance from the metal-dielectric stratified nanostructures ($d_1 = 5$ nm). Parallel and perpendicular dipole moment orientations with respect to the surface of the silver film were considered in the calculations. We adopted and developed the energy flux method presented by Chance, Prock, and Silbey (CPS model),[20,36,37] in which a precise separation of decay channels is provided to distinctly study the effect of SPs modes on each of the decay rates (see supplementary material). Following the CPS model, the normalized radiative decay rate of an emitting dipole in front of an absorbing plasmonic nanostructure can be obtained as

$$\hat{\gamma}_r^{\perp}(\omega) = q - \frac{3}{2} q \, Im\left( \int_0^1 R^{\perp} e^{-2l_d \hat{d}_1} \frac{u^3}{l_d} du \right), \quad (1)$$

$$\hat{\gamma}_r^{\parallel}(\omega) = q + \frac{3}{4} q Im\left( \int_0^1 [R^{\perp} + (1-u^2)R^{\parallel}] e^{-2l_d \hat{d}_1} \frac{u^3}{l_d} du \right). \quad (2)$$

Here, $q$ is the intrinsic quantum yield of the emitting dipole, $\hat{d}_1$ is the normalized dipole distance to the nearest metal

surface, $l_d \equiv -i\sqrt{1 - u^2}$ where $u$ is the integral variable, and $R^{\parallel}$ and $R^{\perp}$ are the near-field reflection coefficients, which are evaluated by defining the Hertz vectors at each layer and applying appropriate boundary conditions at the metal-dielectric interfaces for the parallel and perpendicular dipoles. It is worth mentioning that the near-field reflection coefficients here are a function of the metal films/spacer layer thickness and refractive index, which accordingly allows us to modify the radiative rates by adjusting these variable parameters as long as the experimental limitations are not violated. In the sample fabrication, since the nanoisland formation and consequently high surface roughness are inevitable in the deposition of silver films with the thickness of less than 20 nm,[37,38] for both silver films in the cascaded plasmonic nanostructure, a 20 nm thickness was chosen. This choice results in an effective option to avoid unnecessary metal film absorption in thicker configurations. Taking into account the mentioned practical considerations and for the sake of simplicity, we establish our calculations based on the spacer layer thickness modification (see supplementary material). Figure 1(b) shows the normalized radiative decay rate of an isotropic dipole [$\hat{\gamma}_r^{iso}(\omega) = \hat{\gamma}_r^{\perp}(\omega) + 2/3 \, \hat{\gamma}_r^{\parallel}(\omega)$] with respect to the maximum rate for the stratified structure with its spacer layer thickness varying from 60 to 160 nm. Notably, one can see that the resonance condition (maximum radiative decay rate) for a desired emission wavelength is attainable by modifying the spacer layer thickness. For instance, the maximum radiative decay rate at a dipole peak emission wavelength of 525 nm occurs in the cascaded nanostructure with a spacer layer thickness of 100 nm. This is altered to 140 nm for an emitting dipole with an emission wavelength of 600 nm. Such spectral tunability arising from the engineering of the density of states and the efficient coupling of surface mode to the far-field emission through the

stratified structure can be also verified by electric field mapping across the layers [Figs. 1(c)–1(f)]. Two-dimensional full-wave electromagnetic simulation was used to illustrate the field distribution for an emitting dipole through the stratified structure with spacer layer thicknesses of 20, 60, 100, and 140 nm. The initially excited dipole was placed at the centre of top half-space, and its emission wavelength was taken to be 525 nm. The vertical component of the electric field was monitored across all metallic and dielectric layers to perfectly illustrate the SP coupling modification as a function of the spacer layer thickness. Interestingly, substantial electric field enhancement at the dipole position and across all the layers has been observed in the stratified structure with TPBi = 100 nm, which is a distinct consequence of dipole near-field resonance coupling with the far-field modes of the optimized stratified structure. In other words, the constructive interference gives rise to the highest electric field oscillation at the dipole position and the strongest SP mode coupling at each of the metal-dielectric interfaces. Confirming the corresponding results from the radiative decay rate calculations, an excellent agreement was achieved with the electric field maps to illustrate the remarkable potential of stratified structures in tuning the decay rates.

Next, we focus on the effects of the cascaded nanostructure and the choice of the spacer layer thickness on the radiative emission power of a dipole. Two regions of interest are considered in the calculations: the upper free space [Fig. 2(a)] and the outermost space [Fig. 2(b)]. Here, the normalized radiative power is taken as the ratio of the radiative power of an emitting dipole in front of the cascaded structure to the dipole radiation in the vicinity of a quartz substrate (see supplementary material). Figure 2(a) shows the

normalized radiative emission for the isotropic dipole as a function of the peak emission wavelength and the spacer layer thickness. As can be clearly seen, the normalized radiative power is highly dependent on the thickness of the spacer layer (TPBi), leading to the precise control of emission intensity for which both the radiative power enhancement and attenuation are achievable at all dipole emission wavelengths by adjusting the spacer thickness. For the Alq3 dipole at a peak emission wavelength of 525 nm, the highest radiative enhancement factor (REF) of 3.2 folds is found at a spacer layer thickness of 105 nm, which is consistent with the maximum radiative decay rate results in Fig. 1(b). Similarly, the transmission power efficiency is obtained as the ratio of the transmitted radiative power through two absorbing metal films and the spacer layer in the stratified structure to the transmitted dipole power in the proximity of a quartz substrate through the nonabsorbing medium [Fig. 2(b)]. The theoretical calculation predicts ∼100% transmission at the optimum spacer layer thickness. The consistency between the results presented in Figs. 1(b) and 2 demonstrates the capability of the stratified plasmonic nanostructure in engineering the radiative channels at any desired emission wavelength. Noting that the effect of external excitation field was not considered in these calculations, the resulting emission enhancement only results from the dipole field modification due to the surface mode variation at the metallic structure. To experimentally investigate these theoretical results, we have designed experimental samples based on the optimal spacer thickness that was obtained from the maximum radiative power enhancement calculation (Fig. 2) for the emission wavelength of 525 nm (Alq3 peak emission wavelength). In addition, two control samples with a single silver layer of 20 and 40 nm in thickness were also prepared for the comparison of emissive layer radiation intensities in the cases of single metal film and stratified structure configurations. The excitation was applied from the Alq3 side and the photoluminescence (PL) intensity was measured from either the Alq3 side (radiative power enhancement measurement) or the quartz substrate side (transmission measurement) (see supplementary material for details). Figures 3(a) and 3(b) show the measured PL intensities for the emissive layer on the substrate (reference sample), the stratified structure, and the single-layer structure, for which the PL was collected from the emissive layer and substrate sides of the samples, respectively (indicated by the arrows in the schematics). From Fig. 3(a), one can see that all of the stratified and the single-layer structures show enhancement in the radiative emission compared to the reference sample. However, in the stratified structure, thanks to the most efficient SP coupling across the metal-dielectric interfaces, a 3-fold radiative emission enhancement was observed from the emissive layer, which is almost 2.5 times greater than the best enhancement obtained from the single metal film structures [see Fig. 3(a) black and red lines]. Such enhancement arises from efficient alignment of the emission spectrum with DOS in the optimized stratified structure (TPBi = 100 nm), while in single metal film configurations, the coupling tunability is not available due to the fixed silver film SP spectra. Moreover, almost 100% transparency of the optimized stratified structure at the Alq3 peak emission wavelength can be
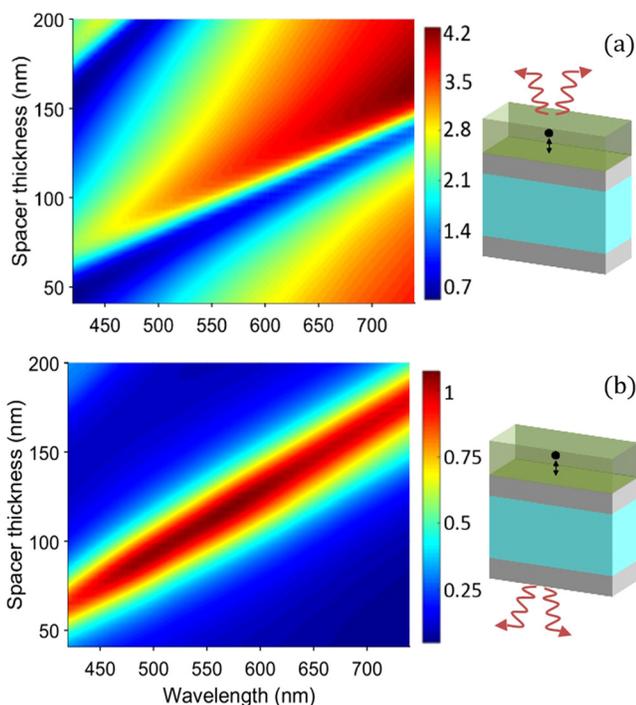


FIG. 2. Calculated radiative power for an isotropic emitting dipole (placed at the distance of $d_1 = 5$ nm from the stratified structure) versus peak emission wavelength and the spacer layer thickness, wherein the radiative power was calculated from (a), the emissive layer and (b), the substrate side of the samples.
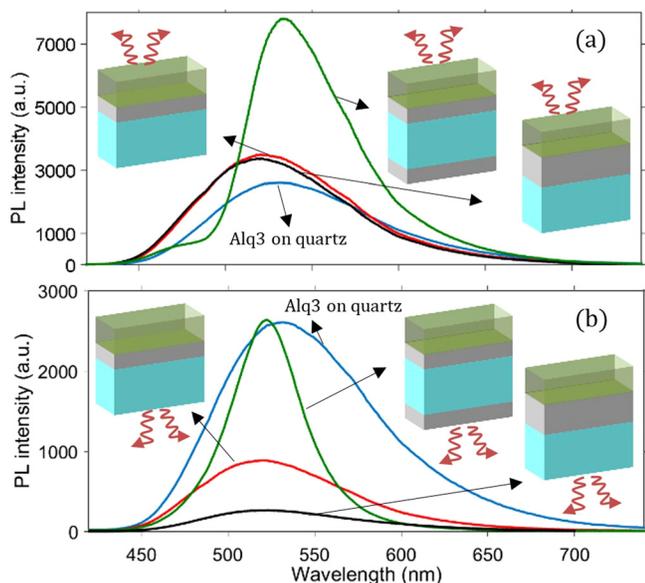
FIG. 3. Photoluminescence intensity measurements radiated from an emissive layer in the front of the stratified structure (green), the single layer configuration with the metal thickness of 20 nm (red), and 40 nm (black) and the Alq3 on the quartz substrate (blue). The thickness of silver film and spacer layer in the stratified structure is 20 nm and 100 nm, respectively.

verified in Fig. 3(b), whereas the single-layer structures with the silver film thicknesses of 20 and 40 nm show only 35% and 10% transparency, respectively. As a result, in the absence of efficient SP resonance coupling, only 10%–12% transmission of dye molecule emission is expected from a stratified structure with two 20 nm-thick metal films, while an optimized thickness of TPBi supports the surface modes at the Ag/TPBi and TPBi/Ag interfaces and results in near-unity transmission at the specific resonance frequency. It is also important to note that the narrower Alq3 emission spectrum with a full-width at half maximum of 50 nm in front of the stratified structure is observed, indicating the spectral filtering behaviour of this plasmonic configuration. Besides the effect of decay rate modification on the emission enhancement, the extinction coefficient of the emitting molecule may profit from the excitation field enhancement. The standing waves that are formed from the reflection of incident excitation field at the interfaces can boost the dye molecule excitation rate. To quantitatively evaluate the experimental results, the radiative enhancement factor (REF) is defined by considering the excitation enhancement in addition to the radiative decay rate in the calculations as follows:

$$REF = \frac{I_{stratified}}{I_0} = \frac{P_{stratified}}{P_0} A_{exciation}, \qquad (3)$$

where $I_{stratified}$ and $I_0$ are the measured PL intensities from the stratified and reference samples, respectively, $P_{stratified}$ and $P_0$ are the calculated emission power through the stratified and reference structures, respectively, and $A_{exciation}$ is the excitation enhancement factor that is calculated at the dipole position at the laser emission wavelength of 405 nm. Figures 4(a) and 4(b) depict REFs that were obtained by the theoretical calculation (solid line), the 2D full-wave simulation (open circle), and the experimental measurements (square) using the stratified structure at the Alq3 peak emission wavelength of 525 nm as a function of the spacer layer thickness varying from 30 to 180 nm. From Fig. 4(a) for which the PL intensities were collected from the emissive layer side, the dependency of REF on the spacer layer thickness can be verified. One may notice that REF can be even smaller than unity (TPBi = 60 nm); however, in most of the cases, the enhancement is greater than one. This behaviour emphasizes the destructive/constructive role of the interference in the stratified configurations changing with the spacer layer thickness and indicates the significance of an optimized design to achieve the resonance matching point at the emission wavelength with the geometrical parameters of the proposed plasmonic structure. Here, note that both the effective excitation cross-section at the dipole position and the decay rate enhancement have been taken into account in the REF calculation presented in Fig. 4. Accordingly, the maximum calculated REF given in Fig. 4(a) is 3.5, while it was obtained to be 3.2 considering only the effect of radiative decay rate [Fig. 2(a)], which confirms a negligible role of the excitation cross-section in our plasmonic configuration.

In summary, we have theoretically and experimentally demonstrated a metal-dielectric-metal stratified structure to tune and enhance the radiative emission rate. We showed that the radiation enhancement reaches a maximum in this stratified architecture with an optimized choice of the spacer layer thickness. A 3-fold radiation enhancement and 100% transmission efficiency, resulting from the stratified structure with a spacer layer thickness of 100 nm for an emitting dipole at the peak emission wavelength of 525 nm, were obtained. Exploiting this effect in active devices such as light-emitting diodes and bio-sensors may hold great promise to enable high efficiency at a targeted operating wavelength.
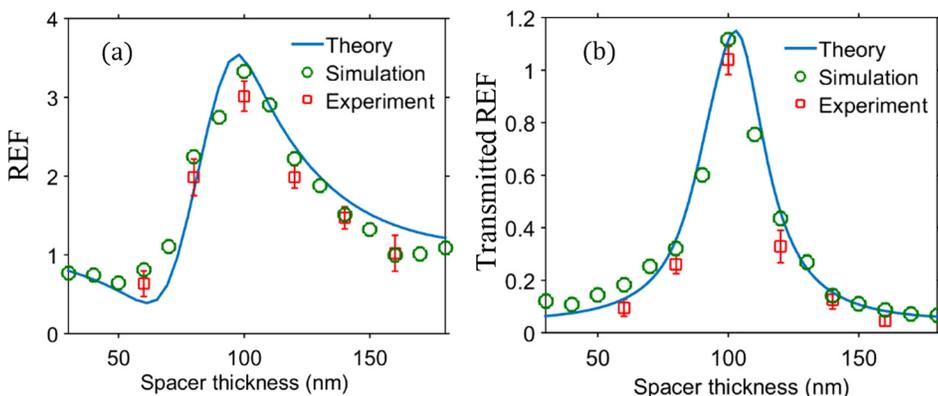


FIG. 4. Radiative enhancement factor (REF) obtained from theoretical calculation (solid line), COMSOL simulation (circle), and experimental measurements (square) using Eq. (3) where the photoluminescence spectra were collected from the emissive layer (a) and the quartz substrate (b) sides of the samples. The emission wavelength in the theoretical calculations and COMSOL simulations is 525 nm.

See supplementary material for theoretical method and simulations used and experimental details.

[1] J. R. Lakowicz, Y. Shen, S. D'Auria, J. Malicka, J. Fang, Z. Gryczynski, and I. Gryczynski, Anal. Biochem. **301**(2), 261–277 (2002).

[2] Y. C. Jun, R. Kekatpure, J. White, and M. Brongersma, Phys. Rev. B **78**(15), 153111 (2008).

[3] W. L. Barnes, A. Dereux, and T. W. Ebbesen, Nature **424**(6950), 824–830 (2003).

[4] K. A. Willets and R. P. Van Duyne, Annu. Rev. Phys. Chem. **58**, 267–297 (2007).

[5] H. Xu, E. J. Bjerneld, M. Käll, and L. Börjesson, Phys. Rev. Lett. **83**(21), 4357 (1999).

[6] K. Diest, J. A. Dionne, M. Spain, and H. A. Atwater, Nano Lett. **9**(7), 2579–2583 (2009).

[7] T. Xu, Y.-K. Wu, X. Luo, and L. Guo, Nat. Commun. **1**, 59 (2010).

[8] S. Akhavan, M. Z. Akgul, P. L. Hernandez Martinez, and H. V. Demir, ACS Nano **11**, 5430–5439 (2017).

[9] S. Golmakaniyoon, H. V. Demir, and X. W. Sun, "Nonradiative energy transfer in a layered metal-dielectric nanostructure mediated by surface plasmons," Proc. SPIE **9547**, 95470T (2015).

[10] S. Golmakaniyoon, P. L. Hernandez-Martinez, H. V. Demir, and X. W. Sun, Sci. Rep. **6**, 34086 (2016).

[11] X. Yang, P. L. Hernandez-Martinez, C. Dang, E. Mutlugun, K. Zhang, H. V. Demir, and X. W. Sun, Adv. Opt. Mater. **3**(10), 1439–1445 (2015).

[12] H. A. Atwater and A. Polman, Nat. Mater. **9**(3), 205–213 (2010).

[13] J. A. Schuller, E. S. Barnard, W. Cai, Y. C. Jun, J. S. White, and M. L. Brongersma, Nat. Mater. **9**(3), 193–204 (2010).

[14] P. A. Hobson, S. Wedge, J. A. Wasey, I. Sage, and W. L. Barnes, Adv. Mater. **14**(19), 1393–1396 (2002).

[15] E. Ozbay, Science **311**(5758), 189–193 (2006).

[16] D. K. Gifford and D. G. Hall, Appl. Phys. Lett. **81**(23), 4315–4317 (2002).

[17] K. Okamoto, I. Niki, A. Shvartser, Y. Narukawa, T. Mukai, and A. Scherer, Nat. Mater. **3**(9), 601–605 (2004).

[18] I. Gryczynski, J. Malicka, Z. Gryczynski, and J. R. Lakowicz, Anal. Biochem. **324**(2), 170–182 (2004).

[19] J. R. Lakowicz, C. D. Geddes, I. Gryczynski, J. Malicka, Z. Gryczynski, K. Aslan, J. Lukomska, E. Matveeva, J. Zhang, R. Badugu, and J. Huang, "Advances in surface-enhanced fluorescence," J. Fluorescence **14**(4), 425–441 (2004).

[20] R. Chance, A. Prock, and R. Silbey, Adv. Chem. Phys. **37**(1), 65 (1978).

[21] W. Barnes, J. Mod. Opt. **45**(4), 661–699 (1998).

[22] S. Gaponenko and D. Guzatov, Chem. Phys. Lett. **477**(4), 411–414 (2009).

[23] P. Törmä and W. L. Barnes, Rep. Prog. Phys. **78**(1), 013901 (2015).

[24] D. Lu, J. J. Kan, E. E. Fullerton, and Z. Liu, Nat. Nanotechnol. **9**(1), 48–53 (2014).

[25] J. Zhang, E. Matveeva, I. Gryczynski, Z. Leonenko, and J. R. Lakowicz, J. Phys. Chem. B **109**(16), 7969–7975 (2005).

[26] O. Muskens, V. Giannini, J. Sanchez-Gil, and J. Gomez Rivas, Nano Lett. **7**(9), 2871–2875 (2007).

[27] K. Shimizu, W. Woo, B. Fisher, H. Eisler, and M. Bawendi, Phys. Rev. Lett. **89**(11), 117401 (2002).

[28] J. R. Lakowicz, Anal. Biochem. **337**(2), 171–194 (2005).

[29] C. Guclu, T. S. Luk, G. T. Wang, and F. Capolino, Appl. Phys. Lett. **105**(12), 123101 (2014).

[30] H. Jia, H. Liu, and Y. Zhong, Sci. Rep. **5**, 8456 (2015).

[31] P. Anger, P. Bharadwaj, and L. Novotny, Phys. Rev. Lett. **96**(11), 113002 (2006).

[32] I. Gontijo, M. Boroditsky, E. Yablonovitch, S. Keller, U. Mishra, and S. DenBaars, Phys. Rev. B **60**(16), 11564 (1999).

[33] J. S. Biteen, N. Pacifici, N. S. Lewis, and H. A. Atwater, Nano Lett. **5**(9), 1768–1773 (2005).

[34] K. Munechika, Y. Chen, A. F. Tillack, A. P. Kulkarni, I. J.-L. Plante, A. M. Munro, and D. S. Ginger, Nano Lett. **10**(7), 2598–2603 (2010).

[35] E. Le Moal, E. Fort, S. Lévêque-Fort, F. Cordelières, M.-P. Fontaine-Aupart, and C. Ricolleau, Biophys. J. **92**(6), 2150–2161 (2007).

[36] R. Chance, A. Prock, and R. Silbey, J. Chem. Phys. **60**(7), 2744–2748 (1974).

[37] R. Chance, A. Prock, and R. Silbey, J. Chem. Phys. **62**(6), 2245–2253 (1975).

[38] K. H. An, M. Shtein, and K. P. Pipe, Opt. Express **18**(5), 4041–4048 (2010).